Regular Article

PHYSICAL CHEMISTRY RESEARCH
Published by the
Iranian Chemical Society
www.physchemres.org
info@physchemres.org

Phys. Chem. Res., Vol. 11, No. 3, 481-491, September 2023
DOI: 10.22036/pcr.2022.345329.2115

An Approach to Increase the Efficiency of Uricase by Computational Mutagenesis

A.K. Nelapati* and K. Meena S
Department of Chemical Engineering, NITK Surathkal, Mangalore, India
(Received 2 June 2022, Accepted 25 July 2022)

Uricase is widely used to treat hyperuricemia and gout. Its clinical use is limited due to side effects such as severe allergy, hypersensitivity, and anaphylactic reactions in some patients. Uricase from *Arthrobacter globiformis (Ag)* and *Bacillus fastidious (Bf)* was chosen to improve enzyme binding energy by reducing the deleterious effects in treatment. To reduce the adverse effects of uricase, enzyme should be modified. For this purpose, we performed *in silico* mutagenesis on uricase. We altered the active site of amino acids of uricase from both sources using f PyMOL. The ligand uric acid was docked with mutated uricase using Autodock 4.0. It was found that mutation of Val64 with Alanine in *Ag* uricase, and mutation of Gly42 with Isoleucine in *Bf* uricase improved the binding energy of the enzyme up to 50%. The binding affinity of native *Ag* uricase docked with uric acid was -8.414 kcal mol^{-1}, while for the mutated enzyme, it was -8.570 kcal mol^{-1}. Binding energies for *Bf* uricase were -5.221 and 5.389 kcal mol^{-1} for native and mutated enzymes, respectively. We showed that our *in silico* model with improved uricase binding energy can facilitate making a potent drug by protein mutagenesis, leading to a drug development with minimum adverse effects to treat hyperuricemia.

Keywords: *Arthrobacter globiformis, Bacillus fastidious*, Docking, Hyperuricemia, *In silico* mutagenesis, Uricase

INTRODUCTION

Uricase or Urate oxidase (EC 1.7.3.3) is an essential enzyme that catalyzes the oxidative breakdown of uric acid to allantoin, H_2O_2, and CO_2, and it is involved in the purine degradation pathway. Allantoin has high solubility, which is more easily excreted compared to urate. It also works as a diagnostic enzyme used to measure urate concentration in urine and blood. Uricase and peroxidase have been used alternatively to determine the concentration of urate [1,2]. Recently the enzyme has also been used for hair coloring [3]. Uricase-based biosensors were developed to detect the level of uric acid [4,5]. Uricase catalyzes the reaction of uric acid as shown in Eq. (1).

$$\text{Uric acid} + H_2O + O_2 \longrightarrow \text{Allantoin} + CO_2 + H_2O_2 \quad (1)$$

*Corresponding author. E-mail: anandaubio@gmail.com

Uricase is present in bacteria, fungi, yeasts, plants, and mammals except humans, due to evolutionary mutations in the uricase gene [6]. This enzyme is located mostly in the liver, and the tetramer is bound to the peroxisome with the subunit of molecular weight 32-33 kDa [7]. Uricase is responsible for the formation of crystalloid core present in the peroxisomes of hepatic cells [8]. Uricase is well known for the treatment of gout arthritis, which is a common type of inflammatory arthritis. The increase in the uric acid concentration in biological fluids (3.6 mg dl^{-1} in child, > 7 mg dl^{-1} in males, and 6 mg dl^{-1} in females) causes a condition known as hyperuricemia in which the accumulation of monosodium urate crystals in the blood causes pain and inflammation in and around joints [9]. One of the reasons of gout in man is the absence of uricase [10]. The administration of uricase leads to a decrease in uric acid plasma levels, which is an alternative treatment for hyperuricemia and gout. Initially, a native enzyme uricase from *Aspergillus flavus* was used to treat hyperuricemia, gout, prophylaxis, and tumor

lysis hyperuricemia. Pegloticase (Krystexxa®, Savient Pharmaceuticals), a PEGylated chimeric porcine-baboon uricase, and Rasburicase (Elitek®, Sanofi-Aventis), a recombinant *Aspergillus flavus* uricase were approved by the US and Europe FDA and used rapidly and safely to decrease plasma uric acid levels dramatically [11]. Rasburicase is an alternative to allopurinol and consists of a single polypeptide chain containing 301 amino acids in *Saccharomyces cerevisiae.* Rasburicase significantly regulates the uric acid concentration faster than allopurinol in clinical trials [12]. Changes in the concentration of uric acid in blood and urine can increase the risk of kidney disease, cardiovascular disease, neurological diseases, hypertension, and stroke [13]. It was also noted that a high concentration of urate was associated with leukemia in children [14]. The drugs have been used for the treatment of these metabolic disorders that induce urinary alkalinization and forced diuresis. Also, xanthine oxidase inhibitors such as allopurinol and febuxostat are used to decrease uric acid synthesis. Uricase produced are mostly antigenic foreign proteins; therefore, frequent medication of uricase results in allergic reactions and anaphylaxis. Allopurinol is a frequently used chemical drug to treat hyperuricemia [15]. Drugs used for decreasing the concentration of uric acid are uric acid synthesis inhibitors (Allopurinol), recombinant uricase preparations, and uricosuric drugs [16].

Docking is an important tool to identify the protein-ligand interaction. It is a method in the field of molecular modelling that estimates the favoured positioning of ligand toward protein when they bound to each other to form a stable complex [17,18]. Docking can determine the binding of a ligand to the protein's binding sites to estimate the small molecule's affinity and putative binding modes. Hence, docking plays an important role in rational drug design [19]. Docking tools such as GOLD, DOCK, ICM, and FlexX are used for high throughput docking simulations. In particular, the efficiency of AutoDock stimulation has been well established in several studies [20,21]. Using computational methods to examine and analyse the binding interactions between proteins and ligands can contribute to drug design [22,23].

Many reports have been reported concerning uricase production by many microorganisms from several sources such as *Nocardifarcinica* [24], *Aspergillus flavus* [25], *Pseudomonas aeruginosa* [26], *Bacillus cereus* [27], *Gliocladium viride* [28], *Streptomyces* [29], and *Candida tropicalis* [30]. Quite a few uricase's three-dimensional crystal structures are available [8,31–33]. Microbial uricases have been recommended for large production over mammalian ones through recombinant expression [34]. The activity and stability of any uricase should be examined for desired applications [35,36]. Up to now, almost all microbial uricases showed minimal enzyme activity and stability under physiological conditions [37,38]. High thermal stability and low activity of *Arthrobacter globiformis* uricase under physiological conditions were reported [39]. Therefore, protein engineering by rational design principles, directed evolution, and a consensus approach is essential to enhance the enzyme activity and uricase thermal stability. The use of medical uricase has been hindered due to its low activity under physiological conditions, short half-life, and limited treatment effect [40]. This enzymatic drug shows allergic, hypersensitivity, and anaphylactic reactions as side effects [41]. Uricase is importance in the clinical field; it is effective in the treatment of hyperuricemia when it has a low Km value and great activity toward uric acid. The modification of uric acid binding site of uricase may result in improved enzyme activity.

Because of uricase's great potential therapeutic value, it is used to treat hyperuricemia, prophylaxis, gout, and tumor lysis hyperuricemia. We designed an *in silico* site-directed mutagenesis of uricase enzyme model sourced particularly from *Arthrobacter globiformis (Ag)* and *Bacillus fastidious (Bf)* in the present study. The bacterial source is the primary source of therapeutic enzymes. The mentioned enzymes were commercialized by Sigma-Aldrich, product numbers U7128 (*Arthrobacter globiformis)* and 94310 (*Bacillus fastidious),* and have been used in several applications [10,42]. Due to high specific activity, *Arthrobacter globiformis* and *Bacillus fastidious* are the main sources of uricase currently employed in therapeutics [42-44]. A few research articles are available on the computational study of uricase from various sources. There are no reports on site-directed mutagenesis of uricase from *Arthrobacter globiformis (Ag)* and *Bacillus fastidious (Bf)*. The docking studies were performed to understand the replacements of which simple amino acid in the substrate uric acid binding site can increase the uricase binding energy.

MATERIALS AND METHODS

Computational Tools Used

The molecular modeling programme ACD/ChemSketch was used to build and change the chemical structures. Also, the software displays molecules and molecular models in two and three dimensions to study the chemical bonding and functional groups [45]. Chemsketch was retrieved from www.acdlabs.com. Before performing the docking, the Openbabel programme was used to change the file to the PDB format [46]. OpenBabel was retrieved from openbabel.org/wiki/Get_Open_Babel. Autodock 4.0 was used to do molecular docking of uricases with uric acid. AutoDock4.0 and Molecular graphics laboratory (MGL) tools were retrieved from mgltools.scripps.edu. From the NCBI PubChem database, the structure of uric acid was found in the form of a spatial data file (SDF). UCSF Chimera was used to observe docked uricase-ligand complexes [47]. The Dock Prep tool of the UCSF Chimera software was used to prepare the ligand and uricase for hydrogen addition, protein optimization, and energy minimization. UCSF Chimera 1.8.1 was retrieved from www.cgl.ucsf.edu. Cygwin (data storage) c:\program was retrieved from www.cygwin.com. PyMOL was used to visualize the proteins, nucleic acids, tiny molecules, electron densities, surfaces, and trajectories in 3D. It edits molecules and traces rays [48]. The PyMOL Molecular Graphics System, Version 2.1.1 Schrödinger, LLC. ASUS (X55OL), CPU (Intel Core i5-4200U, 1.6GHz) system configuration was used.

Retrieval of Protein Targets and their Structure Preparation

The three dimensional structure of *Arthrobacter globiformis* uricase in complex with uric acid (substrate), PDB ID: 2YZB (Method: X-Ray diffraction, Resolution: 1.9 Å, R-value free: 0.223, R-value work: 0.190), and *Bacillus fastidious* uricase, PDB ID:4R8X, Expression system: *Escherichia coli* (Method: X-Ray diffraction, Resolution: 1.401 Å, R-value free: 0.207, R-value work: 0.172), were retrieved from Brookhaven Protein Data Bank (http://www.rcsb.org). Only uricase from *Arthrobacter globiformis* was in complex form with uric acid; before proceeding for docking, uric acid was removed. The mutants were created by utilizing these two structures. Initially, water molecules and bound substrate uric acid were removed from the complex to avoid complexities during docking studies.

Substrate Uric Acid Structure Preparation

The Uric acid ($C_5H_4N_4O_3$) molecular structure was obtained from the PubChem database and designed using the Chemsketch program. The MDL MOL format of the structure was converted into a PDB format file using OpenBabel Software. Further, the PDB structure was used for docking studies.

In Silico Mutagenesis

Active site residues of both the uricase (*Ag* and *Bf*) were investigated by Nelapati *et al.* [49]. The tool PyMOL was used here to modify the enzyme by mutation. Alanine, Leucine, Serine, and Isoleucine, which are simple amino acids, were selected for mutational analysis of each substrate binding site [50]. These simple amino acids were selected based on their structural simplicity. The active site residues of *Ag* were found to be Asp68A, Thr67A, Ala66A, Val65A, Val64A for *Bf* Lys36, Ile40, Phe118, Gly42, Ala117, Glu226, Asp120, Thr39, Tyr116, Phe41, Glu115, and Asn38 [31,33,49]. The structural complexity of mutating amino acids affects the spontaneity of the protein (specifically in the active site).

Molecular Docking

The unmodified and modified *Ag* and *Bf* uricase (with substituted active site residues) proteins were docked to their substrate uric acid. Rigid docking was done to compare the binding energies considering one of the binding pocket amino acids adjustable in flexible dockings that were performed. The binding affinities were checked with the substrate uric acid binding site. Autodock4.0 (http://autodock.scripps.edu/resources/adt) was used for docking simulations of substrate uric acid to the enzyme uricase. It has been reported in literature that conducting docking studies with the use of the ADT tool is the most popular and most reliable among all other tools [51,52]. The graphical user interface ADT was used to set up the two molecules (uricase and uric acid) for docking. The addition of all polar hydrogen atoms, merging non-polar hydrogens, and kollman charges in the manual preparation of the protein are the necessary procedures for the exact determination of partial atomic charges using autodock tools software. Also, gasteiger charges found five aromatic carbons, detected

0 rotatable bonds, and set the number of torsional degrees of freedom (TORSDOF) to 0 in case of ligand. PDBQT structure format of uricase and uric acid were generated by MGL Tools. Grid file and docking file were generated, and the number of grid points in x, y, and z dimensions was set to 80 × 80 × 80 Å for *Ag* and *Bf* specific docking; This was 126 × 126 × 126 Å for *Ag* and *Bf* blind docking for the AutoGrid calculations. The binding pocket residues were placed at the grid box's center with a spacing of 0.375 Å.

The important genetic algorithm parameters were set to both rigid and flexible docking as follows: population size -150, number of GA runs -100, the maximum number of generations -27000, maximum number of evals (medium) -2500000, the maximum number of top individuals (automatically survive) -1, rate of crossover -0.8, gene mutation rate 0.02, GA crossover mode twopt, the variance of Cauchy distribution for gene mutation 1.0, mean of gene mutation Cauchy distribution -0.0, and number of generations (for picking worst individual) -10. The Autodock calculations were done based on a Lamarckian Genetic Algorithm (LGA) in the entire autodock experiment. The structure (uricase-uric acid complex) with the least binding energy (best-docked energy) was chosen from the 100 docked conformational clusters. RMSD cluster analysis was performed based on the ligand atoms only and the structurally similar clusters ranked in order of increasing energy. The estimated binding energy in Autodock is equal to four energies (final intermolecular and electrostatic, final total internal energy, torsional free and unbound system's energy).

RESULTS AND DISCUSSION

Target Uricase

Three-dimensional structures of *Arthrobacter globiformis (Ag)* and *Bacillus fastidious (Bf)* uricase with 2YZB and 4R8X were downloaded in PDB format and are shown in Fig .1.

In silico Mutagenesis

In silico site-directed mutagenesis was performed for each twelve active site residues of uricase from *Ag* and *Bf* with all the four simple amino acids using PyMOL software. The simple structure of amino acids, serine, leucine, alanine, and isoleucine was chosen because the nativity of the protein

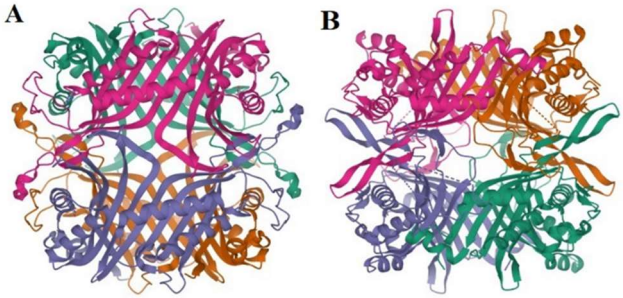

Fig. 1. 3D structures of uricase (A) 2YZB - *Arthrobacter globiformis* (B) 4R8X-*Bacillus fastidious*.

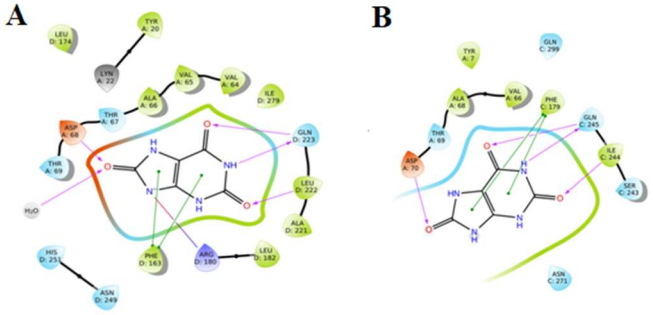

Fig. 2. Native uricase docked with uric acid (A) *Arthrobacter globiformis* (B) *Bacillus fastidious*.

should not be affected, even though *in silico*-directed mutations were performed. Totally, 44 and 46 mutated structural models of *Ag* and *Bf* uricases were obtained, and molecular docking was accomplished to determine the binding energy of the protein. Active site residues for *Ag* and *Bf* are shown in Fig. 2.

Molecular Docking

The obtained results were analysed after the completion of the docking simulation. The lowest binding energy model among the other populated conformations was selected as usual [53,54]. Hydrogen bonds and other details for interactions between uricase and substrate uric acid were examined using PyMOL software. As mentioned in materials and methods, each 12 active site residues from both sources of the native and mutated *Ag* and *Bf* uricase were subjected to blind and flexible docking. The binding energies were computed for both the sources of uricase docked against the substrate uric acid. 100 conformations and their RMSD

values were obtained from the clustering histogram in the molecular docking. The cluster RMSD of 0.00 Å with the least binding energy was chosen from the populated cluster. The substrate uric acid interacted significantly with uricase from *Ag* and *Bf* in the docking grid.

According to results, the blind docking binding energy values of native *Ag* uricase and when native protein was mutated, active sites of Val64 to Ala64, were -5.44 kcal mol^{-1} and -5.78 kcal mol^{-1}, respectively. The flexible docking energies of native *Ag* uricase and mutated protein Val64 to Ala64 were -5.93 and -6.44 kcal mol^{-1}, showing good uricase binding energy (Table 1). Similarly, in the case of native *Bf* uricase, a blind docking score of -6.31 kcal mol^{-1} and -6.41 kcal mol^{-1} was obtained for Gly42 to Ile42 mutation. The flexible docking score of native *Bf* uricase was -6.56 kcal mol^{-1} and that of mutations Gly42 to Ile42 was -6.76 kcal mol^{-1} (Table 2). It is clear from these results that the wild form of the enzyme exhibits less uricase binding energy. In the case of *Ag* uricase, the substitution of val64 with alanine showed the best result. In *Bf* uricase, the substitution of gly42 with isoleucine showed best result with enhanced uricase binding energy. Docking studies showed that specifically the amino acid alanine for *Ag* uricase and isoleucine for *Bf* uricase can be replaced in the binding site to improve the binding energy of the enzyme. It is also found that the mutation of both *Ag* and *Bf* uricase with amino acids serine, leucine, and isoleucine at the active site didn't significantly decrease the uricase binding energy. Therefore, the two simple amino acids, alanine and isoleucine replacements, exhibited the best results among all other residual mutations for obtaining the enzyme with the required characteristics. Finally, LigPlot software, which generates schematic diagrams of protein-ligand interactions, was used to depict a two-dimensional schematic diagram using a PDB input file [55,56]. LigPlot+ (v.2.2.5) was used for the interaction of uric acid with the mutated enzyme that are shown in Fig. 3. The molecular docking results clearly indicate that even after mutating the substrate, active sites with simple amino acids didn't affect the enzyme's binding energy. The quality assessment of each mutant uricase model was passed by the SAVES server. It was confirmed that obtained protein model improved the binding energy without influencing the catalytic function.

Table 1. The Docking Binding Energy Values Results Obtained for both the Wild and Mutated *Arthrobacter Globiformis (Ag)* Uricase in kcal mol^{-1}

2YZB	Active sites	Simple Amino acids	Blind	Specific
Native uricase			-5.44	-5.93
1	ASP 68A	Ala 68	-5.44	-6.02
2		Ser 68	-5.44	-5.99
3		Leu 68	-5.45	-6.03
4		Ile 68	-5.44	-6.12
5	Thr 67A	Ala 67	-5.44	-5.64
6		Ser 67	-5.45	-5.86
7		Leu 67	-5.45	-5.75
8		Ile 67	-5.45	-5.96
9	Ala 66A	Ser 66	-5.45	-5.93
10		Leu 66	-5.45	-5.64
11		Ile 66	-5.43	-5.64
12	Val 65A	Ala 65	-5.45	-5.98
13		Ser 65	-5.44	-5.95
14		Leu 65	-5.44	-5.99
15		Ile 65	-5.45	-5.75
16	Val 64A	Ala 64	-5.78	-6.44
17		Ser 64	-5.45	-6.09
18		Leu 64	-5.45	-5.74
19		Ile 64	-5.44	-6.00
20	Thr 69A	Ala 69	-5.45	-5.97
21		Ser 69	-5.44	-5.92
22		Leu 69	-5.44	-6.00
23		Ile 69	-5.45	-5.64
24	Phe 163D	Ala 163	-5.45	-4.61
25		Ser 163	-5.45	-5.64
26		Leu 163	-5.44	-5.64
27		Ile 163	-5.45	-5.64
28	Leu 222D	Ala 222	-5.44	-5.96
29		Ser 222	-5.44	-5.64
30		Ile 222	-5.51	-6.13
32		Ser 180	-5.44	-5.71
33		Leu 180	-5.45	-5.72

Table 1. Continued

34		Ile 180	-5.45	-5.72
35	Gln 223D	Ala 223	-5.45	-5.64
36		Ser 223	-5.45	-5.64
37		Leu 223	-5.44	-5.64
38		Ile 223	-5.45	-5.64
39	Ala 221D	Ser 221	-5.45	-5.64
40		Leu 221	-5.44	-6.02
41		Ile 221	-5.44	-5.82
42	Ile 279D	Ala 279	-5.45	-5.82
43		Ser 279	-5.44	-5.64
44		Leu 279	-5.45	-6.15

Table 2. Molecular Docking Results Obtained for both the Wild and Mutated *Bacillus Fastidious (Bf)* Uricase in kcal mol^{-1}

4R8X	Active sites	Simple Amino acids	Blind	Specific
Native uricase			-6.31	-6.56
1	Lys36	Ala36	-5.96	-6.32
2		Ser 36	-5.96	-6.10
3		Leu36	-6.15	-6.38
4		Ile36	-6.16	-6.41
5	Ile40	Ala40	-6.29	-6.50
6		Ser40	-6.28	-6.48
7		Leu40	-6.29	-6.51
8	Phe118	Ala118	-6.30	-6.52
9		Ser118	-6.29	-6.51
10		Leu118	-6.36	-6.63
11		Ile118	-6.31	-6.58
12	Gly42	Ala42	-6.35	-6.60
13		Ser42	-6.33	-6.58
14		Leu42	-6.37	-6.67
15		Ile42	-6.41	-6.76
16	Ala117	Ser117	-6.30	-6.55
17		Leu117	-6.32	-6.58
19	Glu226	Ala226	-6.35	-6.60

Table 2. Continued

20		Ser226	-6.35	-6.60
21		Leu226	-6.35	-6.59
22		Ile226	-6.35	-6.59
23	Asp120	Ala120	-6.31	-6.55
24		Ser120	-6.31	-6.56
25		Leu120	-6.31	-6.55
26		Ile120	-6.31	-6.55
27	Thr39	Ala39	-6.32	-6.56
28		Ser39	-6.32	-6.56
29		Leu39	-6.31	-6.56
30		Ile39	-6.31	-6.56
31	Tyr116	Ala116	-6.31	-6.55
32		Ser116	-6.30	-6.54
33		Leu116	-6.31	-6.56
34		Ile116	-6.32	-6.56
35	Phe41	Ala41	-5.97	-5.94
36		Ser41	-5.96	-5.93
37		Leu41	-5.96	-6.28
38		Ile41	-5.97	-6.18
39	Glu115	Ala115	-6.04	-6.22
40		Ser115	-5.97	-6.17
41		Leu115	-5.97	-5.91
42		Ile115	-5.96	-6.04
43	Asn38	Ala38	-5.97	-5.91
44		Ser38	-5.96	-5.93
45		Leu38	-5.96	-5.74
46		Ile38	-6.04	-6.16

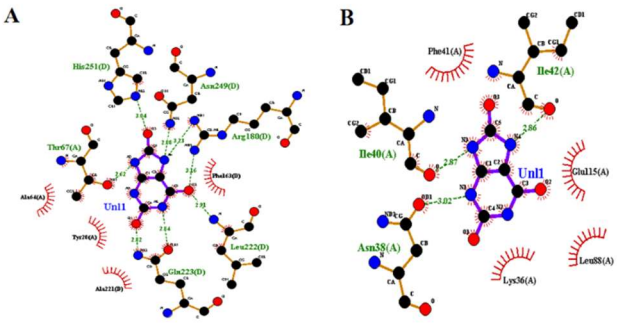

Fig. 3. Binding orientations of mutated uricase enzyme with ligand uric acid (A) Alanine was replaced with Val64 in *Arthrobacter globiformis* (B) Isoleucine was replaced with Gly42 in *Bacillus fastidious*.

Ramya *et al*. [50] studied site-directed mutagenesis to minimize glutaminase side activity of L-Asparaginase from *Pectobacterium carotovorum* to increase its efficiency while treating acute lymphoblastic leukemia by *in silico* approach. Their docking results showed that Asp96 with Alanine had a 30% reduction in the activity of glutaminase and a 40% increase in the activity of asparaginase. Tao *et al.* [57] found that mutation in *candida* uricase improved the catalytic activity of uricase and its polymerization state. Their study proved that Cys249Ser replacement and deletion of C-terminal Leu led to 8% improve in the enzyme activity. Guangrong *et al*. [58] developed chimeric uricase using Exon Replacement and Restoration and Site-Directed Mutagenesis. The mutations of Glu24Asp and Glu83Gly were responsible for the increase in porcine-human uricase activity. Jing *et al.* [59] studied the DNA shuffling of the uricase gene that led to create chimeric uricase. The mutations Gly248Ser and Lys266Phe increased the activity of chimera-62. Nelapati *et al.* [49] showed improved uricase catalytic activity found for Thr159Trp, Asp169Cys, Asn264Trp, and Tyr203Asp mutations in uricase from *Arthrobacter globiformis*, while Ser139Val, Lys215Trp, Gly216Phe, and Ile172Pro mutations in uricase from *Bacillus fastidious.*

CONCLUSIONS

In this work, *in silico* site-directed mutagenesis for designing the potent uricase drug from *Arthrobacter globiformis* and *Bacillus fastidious* were studied. Our goal was to improve the enzyme binding energy and minimize the adverse effects and the inherent disadvantages in the treatment of hyperuricemia and gout. The enzyme drug uricase active site amino acids were mutated. The generated models were docked with the substrate uric acid for the identification of important amino acids that participated in improving the uricase binding energy. The substitution of Alanine with valine64 in *Ag* uricase enhanced the uricase binding energy by 50% compared to the native uricase. For *Bf* uricase, isoleucine was the significant amino acid for the enhancement of uricase binding energy by 50% compared to the native uricase. This *in silico* work paves a way for *in vivo* and *in vitro* experimentation on site-directed mutagenesis to make a potent hyperuricemia drug. Hence, an enzyme with enhanced binding energy is feasible to be employed as a promising drug to treat hyperuricemia.

ACKNOWLEDGMENTS

We are thankful to the National Institute of Technology Karnataka, Surathkal, for providing facilities.

REFERENCES

[1] Pustake, S. O.; Bhagwat, P. K.; Dandge, P. B., Statistical Media Optimization for the Production of Clinical Uricase from *Bacillus subtilis* strain SP6. Heliyon **2019**, *5(5)*, e01756. DOI: 10.1016/ j.heliyon.2019.e01756.

[2] Chiu, Y. -C.; Hsu, T. -S.; Huang, C. -Y.; Hsu, C. -H., Molecular Elucidation of a Urate Oxidase from *Deinococcus radiodurans* for Hyperuricemia and Gout Therapy. *Int. J. Mol. Sci.* **2021**, *22(11)*, 5611. DOI: 10.3390/ijms22115611.

[3] Wang, J.; Zhang, L.; Rao, J.; Yang, L.; Yang, X.; Liao, F., Design of *Bacillus Fastidious* Uricase Mutants Bearing Long Lagging Phases Before Exponential Decreases of Activities Under Physiological Conditions. *Protein J*. **2021**, *40*(5), 765-775. DOI: 10.1007/s10930-021-09999-0.

[4] Tvorynska, S.; Barek, J.; Josypčuk, B. Flow Amperometric Uric Acid Biosensors Based on Different Enzymatic Mini-Reactors: A Comparative Study of Uricase Immobilization. *Sens Actuators B Chem.* **2021**, *344*, 130252. DOI: 10.1016/j.snb.2021.130252.

[5] Nelapati, A. K.; PonnanEttiyappan, J., Computational Analysis of Therapeutic Enzyme Uricase from Different Source Organisms. *Curr Proteomics.* **2020**, *17*(1), 59-77. DOI: 10.2174/ 1570164616666190617165107.

[6] Chiu, Y. -C.; Hsu, T. -S.; Huang, C. -Y.; Hsu, C. -H., Structural and Biochemical Insights into a Hyperthermostable Urate Ooxidase from *Thermobispora Bispora* for Hyperuricemia and Gout Therapy. *Int. J. Biol. Macromol.* **2021**, *188*, 914-923. DOI: 10.1016/j.ijbiomac.2021.08.081.

[7] Wu, X. W.; Lee, C. C.; Muzny, D. M.; Caskey, C. T., Urate Oxidase: Primary Structure and Evolutionary Implications. *Proc. Natl. Acad. Sci.* **1989**, *86*(23), 9412-9416. DOI: 10.1073/pnas.86.23.9412.

[8] Colloc'h, N.; el Hajji, M.; Bachet, B.; L'Hermite, G.; Schiltz, M.; Prangé, T.; Castro, B.; Mornon, J. P., Crystal Structure of the Protein Drug Urate Oxidase-Inhibitor Complex at 2.05 A Resolution. *Nat. Struct. Biol.* **1997**, *4*(11), 947-952. DOI: 10.1038/nsb1197-947.

[9] Nelapati, A. K.; Meena, S.; Singh, A. K.; Bhakta, N.; Ponnan Ettiyappan, J., *In Silico* Structural and Functional Analysis of *Bacillus* Uricases. *Curr Proteomics.* **2021**, *18*(2), 124-142. DOI: 10.2174/1570164617999200512081127.

[10] Nanda, P.; JagadeeshBabu, P. E., Studies on the Site-specific PEGylation Induced Interferences Instigated in Uricase Quantification Using the Bradford Method. *Int. J. Pept. Res. Ther.* **2016**, *22*, 399-406. DOI: 10.1007/s10989-016-9518-8.

[11] Gabison, L.; Prangé, T.; Colloc'h, N.; El Hajji, M.; Castro, B.; Chiadmi, M. Structural Analysis of Urate Oxidase in Complex with Its Natural Substrate Inhibited by Cyanide: Mechanistic Implications. *BMC Struct Biol.* **2008**, *8*(1), 32. DOI: 10.1186/1472-6807-8-32.

[12] Zhu, T.; Chen, H.; Yang, L.; Liu, Y.; Li, W.; Sun, W. Characterization and Cys-Directed Mutagenesis of Urate Oxidase from *Bacillus Subtilis* BS04. *Biologia*. **2022**, *77*(1), 291-301. DOI: 10.1007/s11756-021-00941-4.

[13] Roopa, R. A.; Mantelingu, K.; Guin, M.; Thimmaiah, S. B., Bienzymatic Spectrophotometric Method for Uric Acid Estimation in Human Serum and Urine. *J. Anal. Chem*. **2022**, *77*(3), 301-307. DOI: 10.1134/S1061934822030091.

[14] Sandhyarani, K.; Madhuri, D.; Ravikumar, Y., Review -Gout In Chicken. *Adv. Anim. Vet. Sci.* **2021**, *10*(3), 702-711. DOI: 10.17582/journal.aavs/2022/10.3.702.711.

[15] Beedkar, S. D.; Khobragade, C. N.; Bodade, R. G.; Vinchurkar, A. S., Comparative Structural Modeling and Docking Studies of Uricase: Possible Implication in Enzyme Supplementation Therapy for Hyperuricemic Disorders. *Comput. Biol. Med*. **2012**, *42*(6), 657-666. DOI: 10.1016/j.compbiomed.2012.03.001.

[16] Zhao, Y.; Yang, X.; Li, X.; Bu, Y.; Deng, P.; Zhang, C.; Feng, J.; Xie, Y.; Zhu, S.; Yuan, H.; Yu, M.; Liao, F., Reversible Inactivation of an Intracellular Uricase from *Bacillus Fastidiosus via* Dissociation of Homotetramer into Homodimers in Solutions of Low Ionic Strength. *Biosci. Biotechnol. Biochem*. **2009**, *73*(9), 2141-2144. DOI: 10.1271/bbb.90347.

[17] Cavasotto, C. N.; Abagyan, R. A., Protein Flexibility in Ligand Docking and Virtual Screening to Protein Kinases. *J. Mol. Biol.* **2004**, *337*(1), 209-225. DOI: 10.1016/j.jmb.2004.01.003.

[18] Amiri, M.; Fazli, M.; Ajloo, D., QSAR, Docking and Molecular Dynamics Studies on the Piperidone-grafted Mono- and Bis-spiro-oxindole-hexahydropyrrolizines as Potent Butyrylcholinesterase Inhibitors. *Phys. Chem. Res.,* **2018**, *6*(4), 685-711. DOI: 10.22036/pcr.2018.109597.1438.

[19] Kitchen, D. B.; Decornez, H.; Furr, J. R.; Bajorath, J., Docking and Scoring in Virtual Screening for Drug Discovery: Methods and Applications. *Nat Rev Drug Discov.* **2004**, *3*(11), 935-949. DOI: 10.1038/nrd1549.

[20] Collignon, B.; Schulz, R.; Smith, J. C.; Baudry, J., Task-Parallel Message Passing Interface Implementation of Autodock4 for Docking of Very Large Databases of Compounds Using High-Performance Super-Computers. *J Comput Chem*. **2011**, *32*(6), 1202-1209. DOI: 10.1002/jcc.21696.

[21] Madeswaran, A.; Umamaheswari, M.; Asokkumar, K.; Sivashanmugam, T.; Subhadradevi, V.; Jagannath, P., *In Silico* Docking Studies of Phosphodiesterase Inhibitory Activity of Commercially Available Flavonoids. *Orient. Pharm. Exp. Med.* **2012**, *12*(4), 301-306. DOI: 10.1007/s13596-012-0071-5.

[22] Moeinpour, F.; Mohseni-Shahri, F. S.; Malaekeh-Nikouei, B.; Nassirli, H., Investigation into the Interaction of Losartan with Human Serum Albumin and Glycated Human Serum Albumin by Spectroscopic and Molecular Dynamics Simulation Techniques: A Comparison Study. *Chem. Biol. Interact.* **2016**, *257*, 4-13. DOI: 10.1016/j.cbi.2016.07.025.

[23] Mohseni-Shahri, F. S.; Moeinpour, F.; Malaekeh-Nikouei, B.; Nassirli, H., Combined Multispectroscopic and Molecular Dynamics Simulation Investigation on the Interaction between Cyclosporine A and β-Lactoglobulin. *Int. J. Biol. Macromol*. **2017**, *95*, 1-7. DOI: 10.1016/j.ijbiomac.2016.10.107.

[24] Ishikawa, J.; Yamashita, A.; Mikami, Y.; Hoshino, Y.; Kurita, H.; Hotta, K.; Shiba, T.; Hattori, M., The Complete Genomic Sequence of *Nocardia Farcinica* IFM 10152. *Proc. Natl. Acad. Sci*. **2004**, *101*(41), 14925-14930. DOI: 10.1073/pnas.0406410101.

[25] Leplatois, P.; Le Douarin, B.; Loison, G., High-Level Production of a Peroxisomal Enzyme: *Aspergillus Flavus* Uricase Accumulates Intracellularly and Is Active in *Saccharomyces Cerevisiae*. *Gene* **1992**, *122*(1), 139-145. DOI: 10.1016/0378-1119(92)90041-M.

[26] Shaaban, M. I.; Abdelmegeed, E.; Ali, Y. M., Cloning, Expression, and Purification of Recombinant Uricase Enzyme from *Pseudomonas Aeruginosa* Ps43 Using *Escherichia Coli*. *J. Microbiol. Biotechnol.* **2015**, *25*(6), 887-892. DOI: 10.4014/jmb.1410.10041.

[27] Khade, S. M.; Srivastava, S. K.; Kumar, K.; Sharma, K.; Goyal, A.; Tripathi, A. D., Optimization of Clinical Uricase Production by *Bacillus Cereus* under Submerged Fermentation, Its Purification and Structure Characterization. *Process Biochem*. **2018**, *75*, 49-58. DOI: 10.1016/j.procbio.2018.09.010.

[28] Nanda P.; PonnanEttiyappan, J., Jenifer Fernandes, Pranita Hazarika. Studies on Production, Optimization and Purification of Uricase from *Gliocladium viride*. *Res. Biotechnol.* **2012**, *3*(4), 35-46.

[29] Watanabe, Y.; Yano, M.; Fukumoto, J., Studies on the Formation of Uricase by *Streptomyces:* Part I. The Effect of Purine Bases on the Induced Formation of Uricase by the Cultured Cells. *Agric. Biol. Chem.* **1969**, *33*(9), 1282-1290. DOI: 10.1080/00021369.1969.10859469.

[30] Tanaka, A.; Yamamura, M.; Kawamoto, S.; Fukui, S. Production of Uricase by *Candida Tropicalis* Using N-Alkane as a Substrate. *Appl. Environ. Microbiol.* **1977**, *34*(4), 342-346. DOI: 10.1128/aem.34.4.342-346.1977.

[31] Juan, E. C. M.; Hoque, M. M.; Shimizu, S.; Hossain, M. T.; Yamamoto, T.; Imamura, S.; Suzuki, K.; Tsunoda, M.; Amano, H.; Sekiguchi, T.; Takénaka, A., Structures of *Arthrobacter Globiformis* Urate Oxidase-Ligand Complexes. *Acta Crystallogr. D Biol. Crystallogr*. **2008**, *64*(8), 815-822. DOI: 10.1107/S0907444908013590.

[32] Oksanen, E.; Blakeley, M. P.; El-Hajji, M.; Ryde, U.; Budayova-Spano, M., The Neutron Structure of Urate Oxidase Resolves a Long-Standing Mechanistic Conundrum and Reveals Unexpected Changes in Protonation. *PLoS ONE.* **2014**, *9*(1), e86651. DOI: 10.1371/journal.pone.0086651.

[33] Feng, J.; Wang, L.; Liu, H.; Yang, X.; Liu, L.; Xie, Y.; Liu, M.; Zhao, Y.; Li, X.; Wang, D.; Zhan, C.-G.; Liao, F., Crystal Structure of *Bacillus Fastidious* Uricase Reveals an Unexpected Folding of the C-Terminus Residues Crucial for Thermostability under Physiological Conditions. *Appl. Microbiol. Biotechnol.* **2015**, *99*(19), 7973-7986. DOI: 10.1007/s00253-015-6520-6.

[34] Khaleghi, R.; Asad, S., Heterologous Expression of Recombinant Urate Oxidase Using the Intein-Mediated Protein Purification in Pichia Pastoris. *3 Biotech.* **2021**, *11*(3), 120. DOI: 10.1007/s13205-021-02670-6.

[35] Nagal, V.; Kumar, V.; Khan, M.; AlOmar, S. Y.; Tripathy, N.; Singh, K.; Khosla, A.; Ahmad, N.; Hafiz, A. K.; Ahmad, R., A Highly Sensitive Uric Acid Biosensor Based on Vertically Arranged ZnO Nanorods on a ZnO Nanoparticle-Seeded Electrode. *New J. Chem*. **2021**, *45*(40), 18863-18870. DOI: 10.1039/D1NJ03744G.

[36] Schlesinger, N.; Padnick-Silver, L.; LaMoreaux, B., Enhancing the Response Rate to Recombinant Uricases in Patients with Gout. *BioDrugs* **2022**, *36*(2), 95-103. DOI: 10.1007/s40259-022-00517-x.

[37] Liu, Z.; Lu, D.; Li, J.; Chen, W.; Liu, Z., Strengthening Intersubunit Hydrogen Bonds for Enhanced Stability of Recombinant Urate Oxidase from *Aspergillus Flavus*: Molecular Simulations and Experimental Validation. *Phys. Chem. Chem. Phys.* **2009**, *11*(2), 333-340. DOI: 10.1039/B811496J.

[38] Zhou, Z.; Zhao, H.; Zhang, L.; Xie, Q.; Liu, Q.; Tong, M.; Yu, X.; Xiong, S., Soluble Expression of Bioactive

Recombinant Porcine-Human Chimeric Uricase Mutant Employing MBP-SUMO Fusion System. *Protein Expr. Purif.* **2022**, *189*, 105978. DOI: 10.1016/j.pep.2021.105978.

[39] Liu, D.; Yang, P.; Wang, F.; Wang, C.; Chen, L.; Ye, S.; Dramou, P.; Chen, J.; He, H., Study on Performance of Mimic Uricase and Its Application in Enzyme-Free Analysis. *Anal Bioanal Chem.* **2021**, *413*(26), 6571-6580. DOI: 10.1007/s00216-021-03620-0.

[40] Taherimehr, Z.; Zaboli, M.; Torkzadeh-Mahani, M., New Insight into the Molecular Mechanism of the Trehalose Effect on Urate Oxidase Stability. *J. Biomol. Struct. Dyn*. **2022**, *40*(4), 1461-1471. DOI: 10.1080/07391102.2020.1828167.

[41] Li, Z.; Hoshino, Y.; Tran, L.; Gaucher, E. A., Phylogenetic Articulation of Uric Acid Evolution in Mammals and How It Informs a Therapeutic Uricase. *Mol. Biol. Evol.* **2022**, *39*(1), msab312. DOI: 10.1093/molbev/msab312.

[42] Punnappuzha, A.; PonnanEttiyappan, J.; Nishith, R. S.; Hadigal, S.; Pai, P. G., Synthesis and Characterization of Polysialic Acid-Uricase Conjugates for the Treatment of Hyperuricemia. *Int. J. Pept. Res. Ther.* **2014**, *20*(4), 465-472. DOI: 10.1007/s10989-014-9411-2.

[43] Tan, Q.; Zhang, J.; Wang, N.; Li, X.; Xiong, H.; Teng, Y., Uricase from B*acillus Fastidious* Loaded in Alkaline Enzymosomes: Enhanced Biochemical and Pharmacological Characteristics in Hypouricemic Rats. *Eur. J. Pharm. Biopharm.* **2012**, *82*(1), 43-48. DOI: 10.1016/j.ejpb.2012.06.002.

[44] Zhao, Y.; Zhao, L.; Yang, G.; Tao, J.; Bu, Y.; Liao, F., Characterization of Uricase from *Bacillus Fastidious* A.T.C.C. 26904 and its Application to serum Uric Acid Assay by a Patented Kinetic Uricase Method. *Biotechnol. Appl. Biochem*. **2006**, *45*(2), 75-80. DOI: 10.1042/BA20060028.

[45] Hunter, A. D., ACD/ChemSketch 1.0 (freeware); ACD/ChemSketch 2.0 and its Tautomers, Dictionary, and 3D Plug-ins; ACD/HNMR 2.0; ACD/CNMR 2.0. *J. Chem. Educ.* **1997**, *74*, 8, 905-906. DOI: 10.1021/ed074p905.

[46] O'Boyle, N. M.; Banck, M.; James, C. A.; Morley, C.; Vandermeersch, T.; Hutchison, G. R., Open Babel: An open chemical toolbox. *J. Cheminform.* **2011**, *7*, 3, 33. DOI: 10.1186/1758-2946-3-33.

[47] Pettersen, E. F.; Goddard, T. D.; Huang, C. C.; Couch, G. S.; Greenblatt, D. M.; Meng, E. C., UCSF Chimera-A Visualization System for Exploratory Research and Analysis. *J. Comput. Chem.* **2004**, *25*(13), 1605-1612. DOI: 10.1002/jcc.20084.

[48] Yuan, S.; Chan, H. C. S.; Hu, Z., Using PyMOL as a Platform for Computational Drug Design. *WIREs Comput. Mol. Sci.* **2017**, *7*(2), e1298. DOI: 10.1002/wcms.1298.

[49] Nelapati, A. K.; Das, B. K.; Ponnan Ettiyappan, J. B.; Chakraborty, D., *In-Silico* Epitope Identification and Design of Uricase Mutein with Reduced Immunogenicity. *Process Biochem.* **2020**, *92*, 288-302. DOI: 10.1016/j.procbio.2020.01.022.

[50] Ln, R.; Doble, M.; Rekha, V. P. B.; Pulicherla, K. K., *In Silico* Engineering of L-Asparaginase to Have Reduced Glutaminase Side Activity for Effective Treatment of Acute Lymphoblastic Leukemia: *J. Pediatr Hematol Oncol.* **2011**, *33*(8), 617-621. DOI: 10.1097/MPH.0b013e31822aa4ec.

[51] Hetényi, C., van der Spoel D. Efficient Docking of Peptides to Proteins without Prior Knowledge of the Binding Site. *Protein Sci.* **2009**, *11*(7), 1729-37. DOI: 10.1110/ps.0202302.

[52] Sousa, S. F.; Fernandes, P. A.; Ramos, M. J., Protein-Ligand Docking: Current Status and Future Challenges. *Proteins.* **2006**, *65*(1), 15-26. DOI: 10.1002/prot.21082.

[53] Matin, M. M.; Chakraborty, P.; Alam, M. S.; Islam, M. M.; Hanee, U., Novel Mannopyranoside Esters as Sterol 14α-demethylase Inhibitors: Synthesis, PASS Predication, Molecular Docking, and Pharmacokinetic Studies. *Carbohydr. Res*. **2020**, *496*, 108130. DOI: 10.1016/j.carres.2020.108130.

[54] Matin, P.; Matin, M. M.; Rahman, M. R.; Kumer, A., Synthesis, Antifungal Activity, and Molecular Docking Studies of Some New Di-O-Isopentanoyl Glucopyranosides. *Phys. Chem. Res.,* **2023**, *11*(1), 149-57. DOI: 10.22036/PCR.2022.334577.2057.

[55] Sheikh-Jalali, H.; Mohseni-Shahri, F. S.; Moeinpour, F., Evaluation of Binding Properties of Bovine Serum Albumin and Pyrimidine Ligand: Spectroscopic and

Molecular Docking Approach. *J.Mol. Struct.* **2022**, 1252, 132222. DOI: 10.1016/j.molstruc.2021.132222.

[56] Mohseni-Shahri, F. S.; Moeinpour, F., Study on the Molecular Interaction of Anthocyanin-rich Eggplant Extracts with Bovine α-Lactalbumin. *Phys. Chem. Res.,* **2022**, *10*(4), 485-494. DOI: 10.22036/ PCR.2022.320439.2004.

[57] Tao, L.; Li, D.; Li, Y.; Shi, X.; Wang, J.; Rao, C., Designing a Mutant Candida Uricase with Improved Polymerization State and Enzymatic Activity. *Protein Eng. Des. Sel.* **2017**, *30*(11), 753-759. DOI: 10.1093/ protein/gzx056.

[58] Xie, G.; Yang, W.; Chen, J.; Li, M.; Jiang, N.; Zhao, B.; Chen, S.; Wang, M.; Chen, J., Development of Therapeutic Chimeric Uricase by Exon Replacement/Restoration and Site-Directed Mutagenesis. *Int. J. Mol Sci.* **2016**, *17*(5), 764. DOI: 10.3390/ijms17050764.

[59] Chen, J.; Jiang, N.; Wang, T.; Xie, G.; Zhang, Z.; Li, H.; Yuan, J.; Sun, Z.; Chen, J., DNA Shuffling of Uricase Gene Leads to a More “Human like” Chimeric Uricase with Increased Uricolytic Activity. *Int. J. Biol Macromol.* **2016**, *82*, 522-529. DOI: 10.1016/ j.ijbiomac.2015.10.053.